Preprint, March 2019

Evolutionary dynamics and diversification in changing environments

Evgeniia Alekseeva[1]*, Michael Doebeli[2] and Iaroslav Ispolatov[3]*

Abstract
We use adaptive dynamics models to study how changes in the abiotic environment affect patterns of evolutionary dynamics and diversity in evolving communities of organisms with complex phenotypes. The models are based on the logistic competition model and environmental changes are implemented as a temporal change of the carrying capacity as a function of phenotype. We observe that the rate of environmental change is a crucial factor that determines whether the community survives or undergoes extinction. Surviving communities adapt to the changing conditions and converge to new stationary states, producing a diverse spectrum of evolutionary dynamics. In the majority of surviving systems we observe a reduction in the number of species, total population size and phenotypic diversity. However, for some systems with initially low number of species, slow environmental changes appear to be a driver of speciation and generate communities with higher phenotypic diversity. Phenotypes of surviving species generally evolve in the direction of the moving maximum of the carrying capacity. However, species also evolve in various phenotypic directions orthogonal to the motion of the optimum. The intensity of this undirected phenotypic dynamics increases with the rate of environmental changes.

Keywords
Environmental changes — Adaptation — Extinction

[1] *Skolkovo Institute of Science and Technology, Moscow, Russia*
[2] *University of British Columbia, Vancouver, Canada*
[3] *Universidad de Santiago de Chile, Santiago, Chile*
***Corresponding authors**: evg.alekseeva93@gmail.com, jaros007@gmail.com

Abstract
We use adaptive dynamics models to study how changes in the abiotic environment affect patterns of evolutionary dynamics and diversity in evolving communities of organisms with complex phenotypes. The models are based on the logistic competition model and environmental changes are implemented as a temporal change of the carrying capacity as a function of phenotype. We observe that the rate of environmental change is a crucial factor that determines whether the community survives or undergoes extinction. Surviving communities adapt to the changing conditions and converge to new stationary states, producing a diverse spectrum of evolutionary dynamics. In the majority of surviving systems we observe a reduction in the number of species, total population size and phenotypic diversity. However, for some systems with initially low number of species, slow environmental changes appear to be a driver of speciation and generate communities with higher phenotypic diversity. Phenotypes of surviving species generally follow the moving maximum of the carrying capacity. However, species also evolve in various phenotypic directions relative to the motion of the optimum. The intensity of this undirected phenotypic dynamics increases with the rate of environmental changes.

Introduction

Over the past decades, the issue of the impact of changing environmental conditions on species and ecosystems has gained increasing prominence, particularly in the context of global warming (Griggs and Noguer 2002). In some cases consequences of climate change can be dramatic. For instance, the mosaic-tailed rat *Melomys rubicola* became apparently the first species whose extinction occurred as a result of habitat destruction due to sea level rise (Gynther et al. 2016). For the same reason polar bears (*Ursus maritimus*) face starvation and experience muscle atrophy and weight loss (Obbard et al. 2016a,b; Whiteman et al. 2017; Pagano et al. 2018). For hunting, this species relies on sea ice, where seals, their primary source of food, rest and breed. Reduction of ice surfaces forces polar bears to overcome long distances by swimming and strongly bias the balance between anabolism and catabolism, which is critical in arctic conditions (Griffen 2018).

However, the majority of ecosystems are characterized by extensive adaptability. In some of them, changing environmental factors lead to diversity reduction, nevertheless, in general many ecosystems will likely survive. For example, this course of events is currently observed in coral reefs. Increasing temperature and acidification of the ocean water affects the symbiotic relationships between corals and microalgae in such a way that corals expel their endosymbionts and bleach (Pogoreutz et al. 2018). Without benefits of symbiosis, corals experience higher mortality, become more sensitive to diseases, and decline. However, because strains of both host and endosymbiont vary in their sensitivity to higher temperatures, some of them can form a thermo-tolerant symbiosis (LaJeunesse 2002; Baker 2003; Little et al. 2004; Smith et al. 2017; Grottoli et al. 2018). Such examples already exist in zones with extreme temperatures, such as the Arabian / Persian Gulf (PAG) (Baker et al. 2004), hence this symbiotic community can adapt, in principle, to changing environments despite a decrease in diversity of its participants.

In fact, the challenges imposed by changing environments vary widely between ecosystems and between species within ecosystems, as e.g. the warming climate induces a diverse spectrum of interconnected changes in environmental conditions and weather patterns. Besides global climatic changes, there are numerous other examples how anthropogenic activity disturbs ecosystems locally by environmental pollution, poaching, modification of geographical landscapes and many others factors (Laskar et al. 2016). Adaptation to changing environments is also an important topic of research in the context of preventing the development of antibiotic and drug resistance. So, in one way or another, biological populations frequently face changing environment, which is an important force of their evolution.

Adaptation to environmental changes has been the subject of both experimental and theoretical research. A nice example of an experimental study of evolution in artificially created changing environment is the work on gradual bacterial adaptation to increasing doses of antibiotic on a giant Petri dish (Baym et al. 2016). Another example of experimental adaptation to a changing environment was observed in a study of phytoplankton biodiversity in increasingly warm water (Yvon-Durocher et al. 2015). However, the slowness of evolutionary processes on human timescales sets strong restrictions of what can be done in such experiments. Free of this limitation theoretical studies are by far more numerous. For example in (Botero et al. 2015), the authors found that certain types of climatic changes force populations to cross ”tipping points” and to switch from one adaptive strategy to a qualitatively different one, which often leads to extinction despite the successful adaptation in the context of the previously used strategy. Another theoretical study has revealed the influence of genetic variance and spatial dispersal on the success of a given number of competing species subjected to changing conditions (Norberg et al. 2012). The combination of high genetic variance and low spatial dispersal is the most conducive to adaptation and survival of the species under the effect of climatic changes. In (Northfield and Ives 2013), the authors have investigated how coevolution in pairs of species with various types of ecological interactions affects the process of adaptation to environmental changes. They argued that types of coevolution with conflicting interests help species to adapt, whereas types of coevolution with non-conflicting interests enhance the effect of climatic changes.

In this work we take a somewhat different look at the influence of environmental changes on an evolving system. As it is widely reported, the problem with environmental changes is often not so much the actual state of the environmental variable, such as the global temperature or the CO_2 concentration, but the accelerated rates at which these variables change. Thus in this work we investigate how an ecosystem, modelled as a community of interacting and evolving species, reacts to environmental changes of various rates. We focus on the particular case of competing species, ignoring for now other ecological interactions, and consider a diversifying community described by a logistic competition model in which the competition between individuals is controlled by several phenotypic traits. Previously it was shown that in such systems, the dimension of phenotype space affects diversification, with higher dimensions leading to higher diversity (Doebeli and Ispolatov 2017). As a community diversifies from low numbers of species, the rates of evolution and of diversification slow down as the community reaches a saturation level of diversity that the environment can sustain. Higher rates of evolution and diversification can be reactivated only when the level of saturation decreases, which can happen with aromorphosis and an extension of the phenotypic space into higher dimensions, or through catastrophic events, leading to mass extinction. However, it is not known which ecological and evolutionary processes unravel in such a system when external intervention, such as ongoing climate changes, persists indefinitely. A naive guess would be that if the rate of change associated with such an intervention is much smaller than the intrinsic adaptation rate of all species, the relative phenotypic distribution of the species would remain almost intact and all species would synchronously follow the environmental change. Yet it is hard to predict even qualitatively what happens when the rate of environmental changes increases, apart from the ultimate extinction of all species for very fast changes. We therefore performed a systematic study of various ecological and evolutionary indicators of the evolving communities for a wide range of rates of environmental changes.

Methods

The Model

Following (Doebeli and Ispolatov 2017), we study a system that can be populated by a varying number of phenotypic species, each defined by its phenotype $\mathbf{x} = (x_1, ..., x_D)$ in D-dimensional phenotype space. In monomorphic communities consisting of a

single species with phenotype $\mathbf{x}$, the population size of that species at ecological equilibrium is given by the carrying capacity function $K(\mathbf{x})$ of the form

$$K(\mathbf{x}) = \exp\left[-\frac{\sum_{i=1}^{D}(x_i - x_{ci})^4}{4\sigma_K^4}\right], \tag{1}$$

where σ_K determines the width of the carrying capacity. This function has its maximum at the point that we call the centre of the carrying capacity (CCC) $\mathbf{x}_c = (x_{c1}, ..., x_{cD})$. Thus, the population size of a monomorphic population is maximal if that population's phenotype is equal to $\mathbf{x}_c$.

Competition between two phenotypes $\mathbf{x}$ and $\mathbf{y}$ is described by the competition kernel $\alpha(\mathbf{x},\mathbf{y})$, so that the competitive effect of $\mathbf{x}$ on $\mathbf{y}$ is given by

$$\alpha(\mathbf{x},\mathbf{y}) = \exp\left[\sum_{i,j=1}^{D} b_{ij}(x_i - y_i)(x_j - x_{cj}) - \sum_{i=1}^{D}\frac{(x_i - y_i)^2}{2\sigma_i^2}\right]. \tag{2}$$

There are two terms in the exponent of the competition kernel. The first one represents the simplest non-symmetric contribution to the competition that may result in complex evolutionary dynamics (Doebeli and Ispolatov 2014; Ispolatov et al. 2016; Doebeli and Ispolatov 2017). Since we expect that the evolutionary dynamics would unravel around the CCC (which was set equal to zero in (Doebeli and Ispolatov 2014; Ispolatov et al. 2016; Doebeli and Ispolatov 2017)), we explicitly introduce it here, replacing x_j by $(x_j - x_{cj})$. The second term in the exponent is the usual Gaussian competition kernel with width σ_i, reflecting the fact that species that are closer phenotypically compete more strongly with each other than species that are farther apart in phenotype space. In our simulations we used $\sigma_K = 1$ and $\sigma_i = 1/2$ to ensure that the system is able to diversify from the initial state of one species to a community of coexisting phenotypes (Ispolatov et al. 2016; Doebeli and Ispolatov 2017). Also as in (Doebeli and Ispolatov 2017), the coefficients b_{ij} of the non-symmetric part of the competition kernel were chosen randomly from a Gaussian distribution with width 1 and zero mean (see the end of this section for how this was implemented to obtain the simulation results).

Assuming that a community comprises m species with phenotypes $\mathbf{x}_r = (x_{r1}, ..., x_{rD})$ in D-dimensional phenotype space, where $r = 1, \ldots, m$ is the species index, the ecological dynamics of the density N_r of species r is given by the logistic equation

$$\frac{dN_r(t)}{dt} = N_r(t)\left(1 - \frac{\sum_{s=1}^{m}\alpha(\mathbf{x}_s,\mathbf{x}_r)N_s(t)}{K(\mathbf{x}_r)}\right). \tag{3}$$

In the framework of adaptive dynamics (Geritz et al. 1998; Diekmann 2002), evolution occurs when species generate rare mutants with phenotypes that are close to but distinct from the parent phenotype. Mutants compete with the resident population for resources and try to invade it with a per capita growth rate given by the invasion fitness function $f(\mathbf{x}_1, ..., \mathbf{x}_m; \mathbf{x}'_r)$:

$$f(\mathbf{x}_{1,\ldots,m}; \mathbf{x}'_r) = 1 - \frac{\sum_{s=1}^{m}\alpha(\mathbf{x}_s,\mathbf{x}'_r)N_s^*}{K(\mathbf{x}'_r)}, \tag{4}$$

where $\mathbf{x}'_r$ is the phenotype of a mutant occurring in species r. By differentiating the invasion fitness with the respect to the mutant phenotype and evaluating at the resident phenotype, one obtains the selection gradient S_r with components S_{ri}:

$$S_{ri} = \sum_{s=1}^{m} N_s^*\left(-\frac{1}{K(\mathbf{x}_r)}\frac{\partial\alpha(\mathbf{x}_s,\mathbf{x}'_r)}{\partial x'_{ri}}\bigg|_{\mathbf{x}_r=\mathbf{x}'_r} + \frac{\alpha(\mathbf{x}_s,\mathbf{x}_r)}{K^2(\mathbf{x}_r)}\frac{\partial K(\mathbf{x}_r)}{\partial x_{ri}}\right) \tag{5}$$

Adaptive dynamics of the phenotypes in each of the m species in a community is determined by the selection gradient and by the mutational variance-covariance matrix, which describes the rate and size of mutations occurring in each species. For simplicity, we assume here that this matrix is diagonal, and that the elements corresponding to each species are proportional to the current population size of that species. The adaptive dynamics of each phenotypic component x_{ri}, $i = 1, \ldots, D$ and $r = 1, \ldots, m$ is then given by

$$\frac{\partial x_{ri}}{\partial t} = \frac{N_r^*}{K(\mathbf{x}_r)}\sum_{s=1}^{m}\left[\alpha(\mathbf{x}_s,\mathbf{x}_r)N_s^*\left(\sum_{j=1}^{D} b_{ij}(x_{sj} - x_{cj}) - \frac{(x_{si} - x_{ri})}{\sigma_i^2} - (x_{ri} - x_{ci})^3\right)\right], r = 1, \ldots, m;\ i = 1, \ldots, D. \tag{6}$$

Further details of the model, including the procedure allowing species to diversify, are presented in the Appendix, Section 1.

So far, this model is the same as the one in (Ispolatov et al. 2016; Doebeli and Ispolatov 2017). Here, however, we introduce environmental change by assuming that the position of the CCC is changing over time, $\mathbf{x}_c = \mathbf{x}_c(t) = \mathbf{V}_C t$, where $\mathbf{V}_C$ is a vector

of a given length V_C, which is the rate of environmental change. Thus, the maximum of the carrying capacity function is assumed to move in phenotype space at a constant rate V_C, while the general shape of the carrying capacity function, and in particular its width σ_K, stay the same.

In the simulations, environmental change starts once an evolving community has reached a stationary state in the evolutionary dynamics without environmental change (Fig. S1), as described in (Doebeli and Ispolatov 2017). We note that stationarity does not imply that evolution comes to a halt; instead, evolution may be ongoing, but statistical properties such as level of diversity and average evolutionary speed reach equilibrium values. In the following we denote this time as t^*. Thus, in our simulation we prepare 100 "replicas" of the system for every phenotypic dimensionality $D = 1, 2$, and 3, each having a distinct randomly chosen set of coefficients b_{ij} and initial conditions. Each replica is evolved for time t^* to its steady state following the procedure outlined in Appendix, Fig. S1. Then, in every dimensionality $D = 1, 2$, and 3 and for each magnitude of V_C, we perform 100 simulation runs, one for each steady state replica. In each run, a new random direction of $\mathbf{V_C}$ is chosen for the same magnitude V_C. Once started, the environmental change occurs at a constant rate V_C for t^* time units. The results for each D and V_C are averaged over those 100 runs, producing statistical data shown in Fig. 3 for the final state and in Figs 4 and 5 for the time course of adaptation (Appendix, Section 1).

Measuring properties of the system

To analyze the evolving communities, we measured the following system properties at t^*:

1) number of species in the system m_{tot}.

2) total population of the system $N_{tot} = \sum_{r=1}^{m} N_r$.

3) phenotypic diversity of the system σ_{tot}^2 as the average square distance of the phenotypic coordinates of all clusters weighted by their population sizes around the centre of mass of the system $\mathbf{x}^{mc} = (x_1^{mc}, ..., x_D^{mc})$, where

$$x_i^{mc} = \frac{\sum_{r=1}^{m} x_{ri} N_r}{N_{tot}} \tag{7}$$

and

$$\sigma_{tot}^2 = \sum_{i=1}^{D} \frac{\sum_{r=1}^{m} (x_{ri} - x_i^{mc})^2 N_r}{N_{tot}}. \tag{8}$$

The quantity σ_{tot}^2 reflects how widely the phenotypes of the various species are separated from the centre of mass of the system. It is a measure of the phenotypic diversity in a community, but should not be confused with the number of species, since the phenotype distribution in systems with smaller numbers of species can nevertheless have a higher variance if the fewer species are more spread out in phenotype space.

4) fraction of extinct species

$$\rho_{ext} = \frac{m_{sat} - m_{tot}}{m_{sat}}, \tag{9}$$

where m_{sat} is the number of species in saturated communities before the initiation of environmental change.

5) average evolutionary speed V_{ev}, reflecting the intensity of phenotypic changes in the whole system, measured relative to the moving CCC:

$$V_{ev} = \frac{\sum_{r=1}^{m} V_r N_r}{\sum_{r=1}^{m} N_r} \tag{10}$$

where

$$V_r = \frac{\sqrt{\sum_{i=1}^{D} (\Delta x_{ri} - \Delta x_{ci})^2}}{\Delta t}. \tag{11}$$

Here Δx_{ri} and Δx_{ci} are the increments of the ith phenotypic component of the rth species and the moving CCC that occur during the integration time step Δt. The evolutionary speed calculated in this way controls for the effect of species adaptively following the moving CCC, and V_{ev} reflects the intensity of phenotypic evolution in addition to that movement.

6) time of extinction t_{ext} if all species of the system go extinct before time t^* after the onset of environmental change.

There are two basic ways in which the above quantities can be calculated to illustrate system behaviour. First, they can be calculate at the final time t^* after the onset of environmental change for many different systems with the same control

parameters (e.g., the same V_C). For example, one can calculate the average number of coexisting species at time t^*, i.e., the average number of coexisting species at the evolutionary quasi-stationary state, by calculating m_{tot} at $t*$ for many different systems. Second, these quantities can be calculated as a function of time in any given simulation run, usually upon initiating the movement of CCC, i.e., the environmental change. For example, before starting the movement of CCC, $m_{tot} = m_{sat}$, i.e., the number of species at saturation. Once CCC starts to move, m_{tot} may drop or increase, depending on the effect of environmental change on a previously saturated community.

Results

Equilibration of the system before motion of CCC

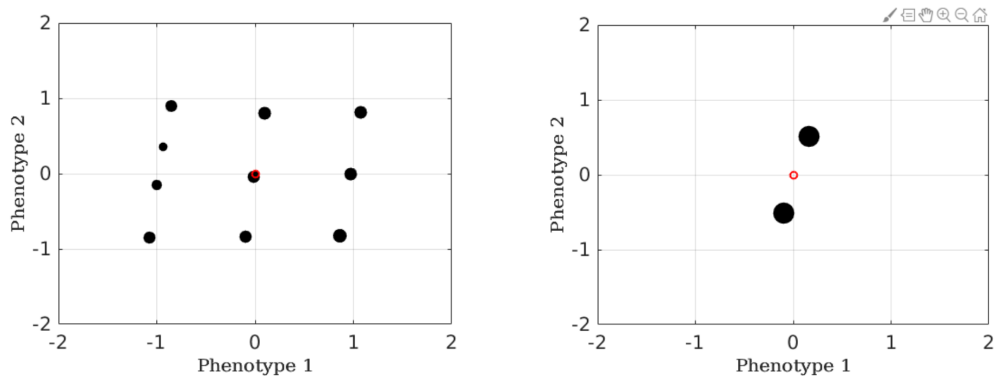

(a) Example of Highly-Saturated System **(b)** Example of Low-Saturated System

Figure 1. Snapshots of system saturation in two-dimensional phenotypic space, $\sigma_K = 1, \sigma_{i=\{1,\ldots,D\}} = 0.5$; the saturation processes that led to these configurations can be seen in videos in Supplementary Fig. S3a and S3b. Here and in the next figure dark grey circles show the location of different species in phenotype space, with the size of the circles representing the populations sizes, the red rhombus shows the location of the CCC. The coefficients b_{ij} and the initial conditions can be found in Appendix, section 2.

We first establish some basic facts about communities evolving in the absence of environmental change. As mentioned in the introduction, such communities reach a quasi-equilibrium state in which the diversity saturates at a certain level and then remains approximately constant thereafter. In fact, depending on parameter b_{ij} in the competition kernel (2), this saturation generally occurs in two qualitatively different forms. The first is a "high-saturation state" (HSS), in which the number of species m_{sat} is large and their phenotypes form an approximately equidistant crystal-like lattice in phenotype space. In such a system, there is very little evolutionary change after the saturation state has been reached (Fig. 1A and Supplementary video Fig. S3A). The second form is a "low saturation state" (LSS), in which the number of species m_{sat} is relatively low and their distribution in phenotype space is sparse. In such a system, diversification also comes to a halt after reaching saturation, but the evolutionary dynamics of the phenotypes of the coexisting species do not reach an equilibrium, and instead exhibits sustained oscillations in phenotype space (Fig. 1B and Supplementary video Fig. S3B). We will see that some of the effects of environmental change in evolving communities are different for HSS and LSS systems.

Adaptation to the CCC motion and convergence to a new quasi-stationary state

Environmental change in the form of a moving CCC either forces the system to adapt and converge to a new quasi-stationary state, or it leads to extinction of the whole community. In the former case, the process of adaptation appears to be different depending on the initial level of the community's saturation at the onset of environmental change, and on the rate of environmental change, V_C. Upon initiation of the environmental change, i.e., the movement of CCC, high-saturation (HSS) systems always loose some species, and the amount of species loss depends on V_C. HSS systems change their phenotypic composition, so that the remaining species form a community with increased rates of evolution relative to the the motion of CCC. This is illustrated in Fig. 2A and and Supplementary video Fig. S4A. In low-saturation (LSS), similar effects can be seen. However, in LSS systems low rates of environmental change V_C can be a driver of diversification: due to the movement of CCC, LSS systems can break out of their low-saturation, periodic evolutionary dynamics and undergo new bouts of diversification, potentially reaching higher levels of diversity than before the environmental change was initiated. This is illustrated in Fig. 2B and and Supplementary video Fig. S4B.

Nevertheless, taking the average from 100 simulation runs for each value of V_C, the final number of species m_{tot} (Fig. 3A) and the total population size N_{tot} (Fig. 3D) always decrease with the speed of environmental changes, V_C. For a given value of

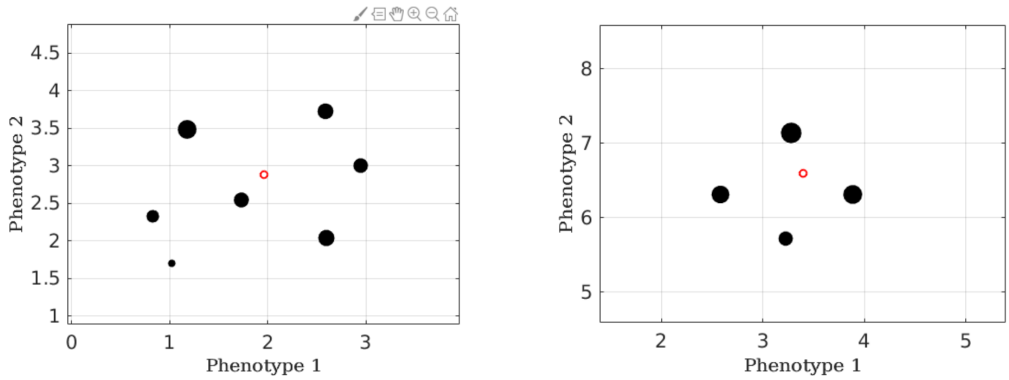

(a) Example of Highly-Saturated System **(b)** Example of Low-Saturated System

Figure 2. Snapshots of system adaptation in two-dimensional phenotypic space, $\sigma_K = 1, \sigma_{i=\{1,\ldots,D\}} = 0.5$; the adaptation processes that led to these configurations can be seen in Supplementary Fig. S4A and S4B, the coefficients b_{ij} and the initial conditions can be found in Appendix, section 2.

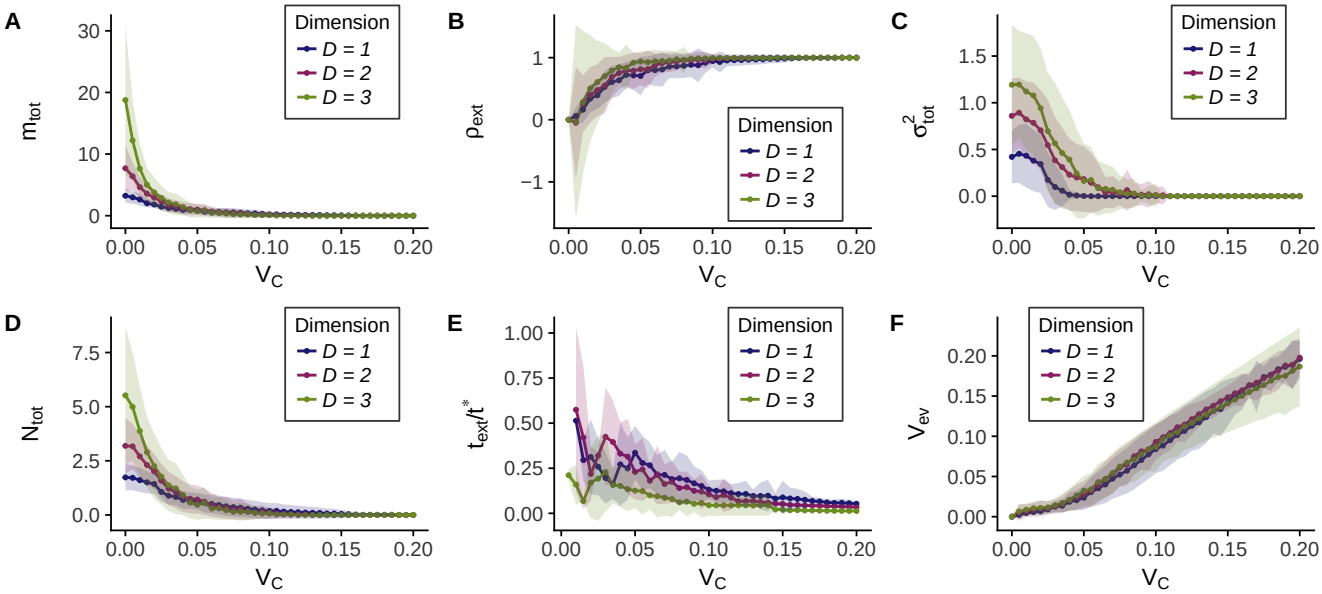

Figure 3. Averaged final system properties as a function of the the speed V_C of the CCC motion. For each value of V_C, quantities were calculated from 100 systems after they evolved with a moving CCC for a period of time t^* after reaching evolutionary quasi-stationarity (except for average time to extinction, which was measured for those communities in which all species went extinct before time t^* after the onset of environmental change). Values of t^* for each dimensionality of the phenotype space can be found in Appendix, Fig. S2. Colour indicates different dimensions of phenotype space: blue for $D = 1$, red for $D = 2$, and green for $D = 3$. Data points represent the mean output of simulations and shadows around lines represent the standard deviation: **A:** number of species in the community, m_{tot} ; **B:** fraction of species that went extinct before time t^*, ρ_{ext}; **C:** phenotypic variation across the community, σ^2_{tot}; **D:** total population size of the community, N_{tot}; **E:** normalized time to total extinction t_{ext}/t^*; **F:** average evolutionary speed in the community at stationary state, V_{ev}, defined in (10).

V_C, these system properties begin to decrease shortly after the onset of environmental change and then stabilize after some time (despite the ongoing CCC movement), as illustrated in Fig. 4. The higher the V_C, the faster this decrease occurs. Typically, the time required to reach a new evolutionarily stationary state is small relative to the saturation time t^*. The higher V_C, the less time is required.

The average value of σ^2_{tot} decreases for increasing V_C as well (Fig. 3C), since larger rates of environmental change cause the loss of more species, however the shape of the decreases is different from that for m_{tot} and N_{tot}. For small values of V_C, the average value of σ^2_{tot} over all communities is larger than the corresponding average for saturated systems before the environmental change. This is due to the generation of new species in low-saturation systems upon environmental change. For

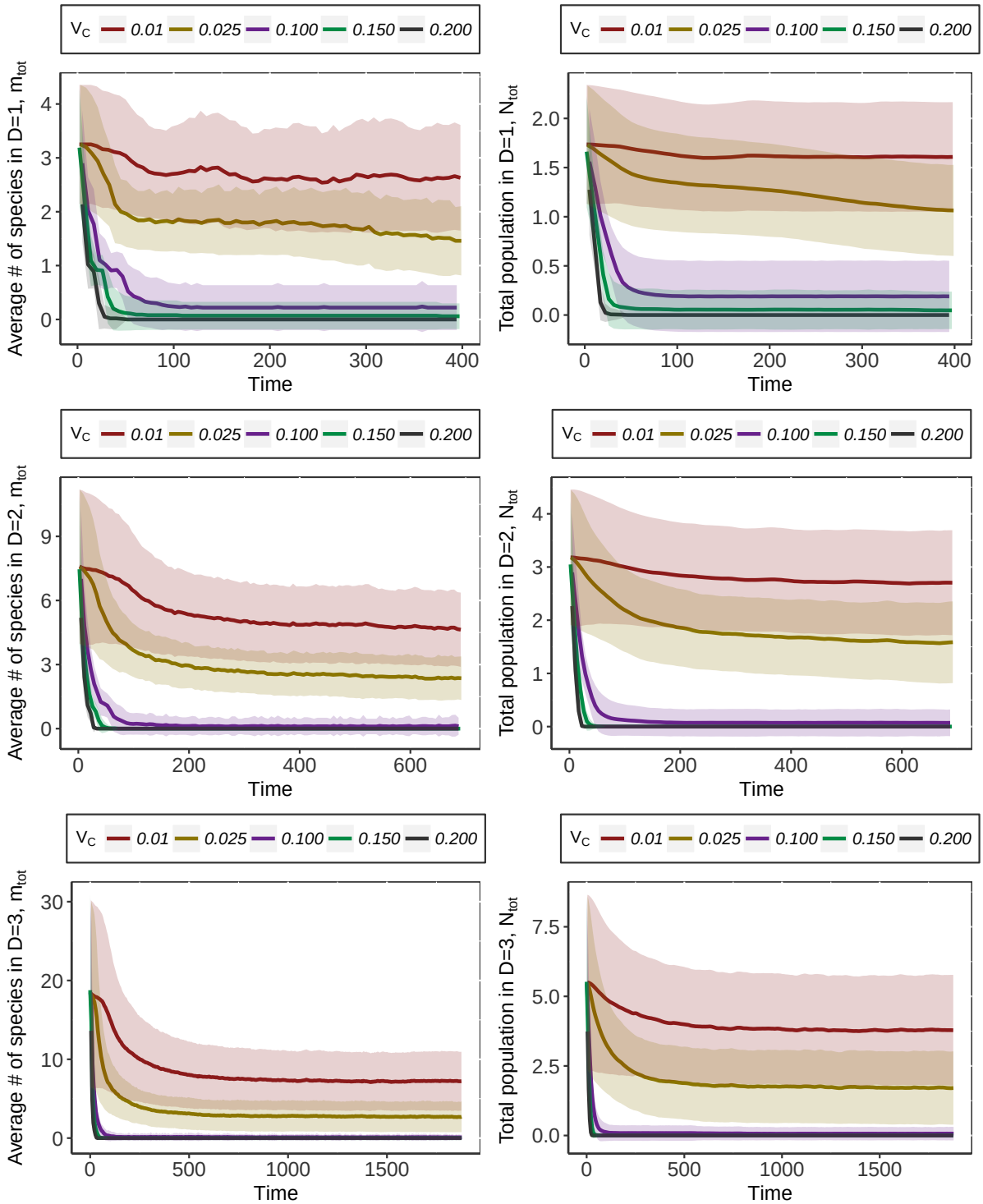

Figure 4. Dynamics of average number of species m_{tot} and total population N_{tot} as a function of time after the onset of environmental change for different values of V_C.

larger values of V_C some evolving communities still exhibit increased phenotypic diversity σ^2_{tot} despite the overall trend, but this increase is not necessarily accompanied by an increase in m_{tot} over m_{sat}, and for such systems an elevated σ^2_{tot} indicates that phenotypic spread of the surviving species around the centre of mass becomes wider (Appendix, Fig. S4). When considering the average square phenotypic distance σ^2_{tot} over the course of individual simulations, σ^2_{tot} first decreases over time after the onset of environmental change and then approaches a stationary state. σ^2_{tot} may stay at the level of saturated system without

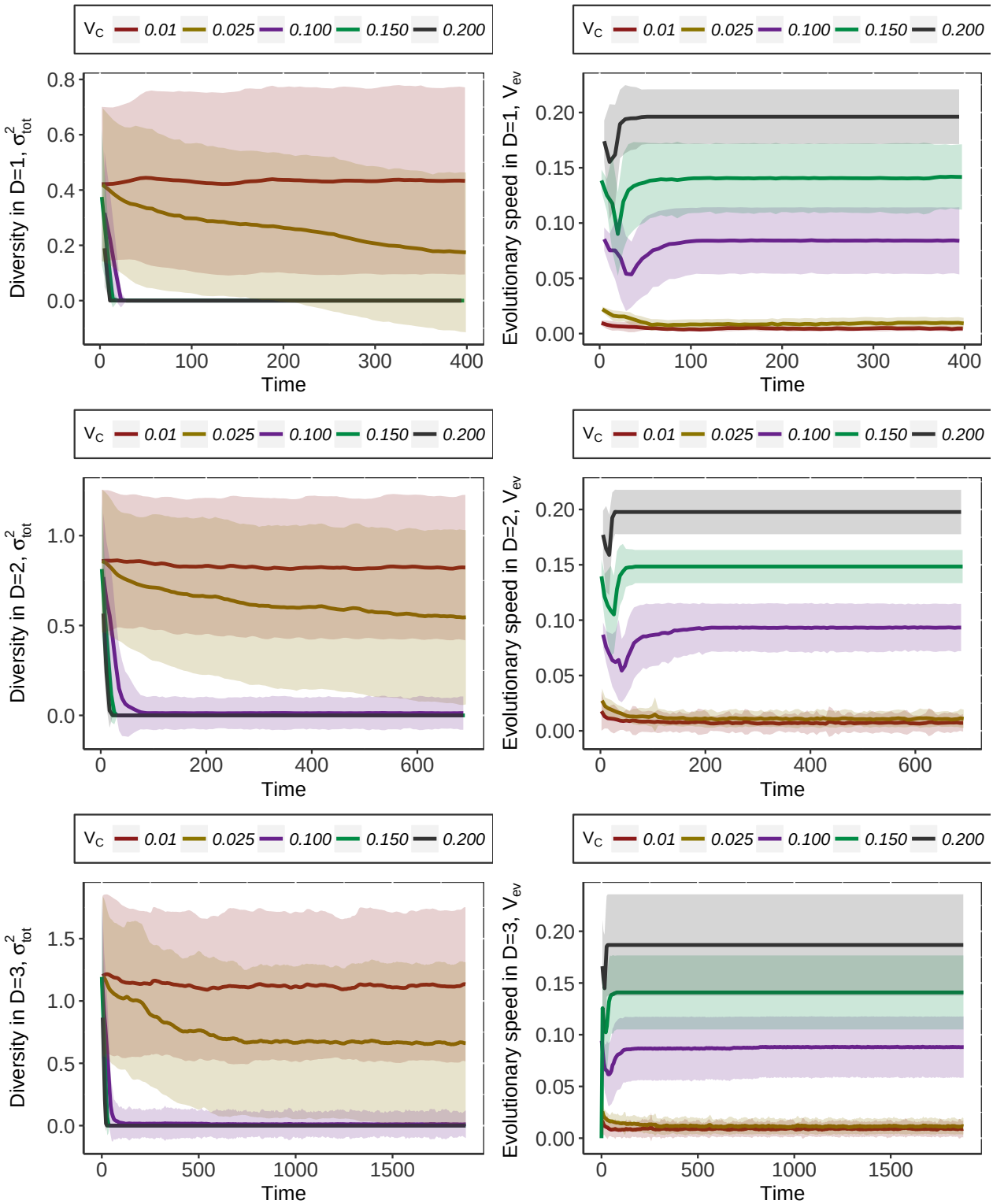

Figure 5. Dynamics of diversity σ^2_{tot} defined in (8 and evolutionary speed V_{ev} defined in (10) as a function of time after the onset of environmental change for different values of V_C.

environmental change or even exceed it in the case of low rates of V_C (Fig. 5).

Conversely, the average fraction of extinct species ρ_{ext} grows (Fig. 3B) with increasing V_C. Here the contribution of LSS systems, where environmental change induces diversification of species, can also be seen, leading e.g. to negative values of ρ_{ext}

for $V_C = 0.005$ in $D = 2$, and to increased widths of the distribution of ρ_{ext} for small values of V_C. The higher the dimensionality of phenotype space, the more diverse outputs the system can produce, as indicated by the shaded regions in the figures, which represent standard deviations of measurements obtained from the simulations.

Evolutionary speed V_{ev} is the rate of evolutionary change in phenotype space relative to the motion of CCC (i.e., controlling for the rate of environmental change). For the moving CCC, the average steady state evolutionary speed increases with increasing rate of environmental change V_C, and this increase appears to be largely independent of the dimension of phenotype space (Fig. 3F). The average evolutionary speed of equilibrated systems before the start of environmental changes has a nonzero value, since LSSs continue to exhibit phenotypic fluctuations even in the stationary state. When the CCC starts to move, the average V_{ev} first dips from its initial level, but then recovers and approaches a stationary value that exceeds the initial speed V_{ev}. The transitory dip can be explained by extinction caused by the moving CCC in a number of systems and subsequent acceleration of evolution in the remaining ones, since an empty system contributes zero to the averaged over 100 systems velocity but is still included when taking averages. The higher V_C, the longer it takes V_{ev} to reach its stationary state (Fig. 5).

Extinct systems

Even at small values of V_C the entire evolving community can go extinct, an event that becomes more likely for increasing rates of environmental changes V_C. In fact, our simulations indicate that for any fixed set of parameters, there is a value of V_C for which extinction becomes certain. We call this value the extinction threshold. Interestingly, this extinction threshold is lower for increased dimensions of phenotype space, presumably because higher dimensional phenotypes make adaptation a more complicated process. A more mechanistic explanation for the observed reduction of the extinction threshold is that in higher dimensions the population N_r of each species is generally smaller. In higher-dimensional systems, each species has on average more competitors due to larger number of "nearest neighbours" with slightly different phenotypes. The smaller population means lower mutation rates and slower adaptation in terms of the dynamics (6), since the adaptation rate of a species is proportional to its population N_r.

The fraction of surviving communities as a function of V_C and the extinction threshold value of V_C are shown in Fig. S3 of the Appendix. Generally, the higher the rate of environmental change, the more likely extinction occurs. Interestingly, despite this obvious general trend, the corresponding times to extinction $t_{ext}/t*$ vary widely and only become very short at large values of V_C, regardless of the dimension of phenotype space (Fig. 3E). This is because whether extinction occurs, and when, strongly depends on the initial steady state configuration of the system and the set of coefficients b_{ij} in the competition kernel.

To check the robustness of these results we have repeated these simulations for fewer than 100 replicas for two other values of the width of the competition kernel, $\sigma_i = 0.25$ and 0.75. Even though the saturated level of diversity varies strongly with σ_i (Doebeli and Ispolatov 2017), the trends shown and Fig. 3, 4, and 5 remain qualitatively unchanged.

Discussion

We have investigated the evolutionary dynamics in logistic competition models under the assumption of gradual environmental change, which was implemented by assuming that the maximum of the carrying capacity function moves at a constant speed in phenotype space. We have analyzed the effect of such environmental change on various statistics calculated in the evolving communities, depending on the rate of the environmental change and on the dimension of phenotype space.

The general gist of our conclusions is not unexpected and fits well with observations from natural systems. With gradual environmental change, the phenotype of a species generally has to evolve in step with the movement of the centre of the carrying capacity, because otherwise the carrying capacity of that species will fall to very low values, making the environment inviable for that species. Such effects can be observed in various populations (Gienapp et al. 2008; Baym et al. 2016; Tseng et al. 2018). For example, numerous studies indicated a global tendency of various species to decrease in body size in warming environments (Guillemain et al. 2005; Y. Yom-Tov and J. Yom-Tov 2005; Y. Yom-Tov and S. Yom-Tov 2006; Y. Yom-Tov, Leader, et al. 2010; Gardner et al. 2011). Body size is an important physiological characteristic that strongly influences metabolism and thermoregulation. For example, decreased body-size due to changing temperature regimes was observed in beetles both in natural and laboratory populations (Tseng et al. 2018).

In our models, the crucial factor determining whether an evolving community will survive in the long run is the rate of environmental change, V_C. We found that there is a threshold value of V_C above which communities cannot survive, and this threshold V_C becomes smaller with increasing dimensionality of the phenotype space. This would indicate that "simpler" organisms and ecosystems can withstand higher rates of environmental change. Below the threshold value, the higher V_C, the lower is the average number of coexisting species m_{tot} and the total population size N_{tot} of surviving communities at evolutionary stationary states.

Our extensive simulations revealed that for V_C above the extinction threshold, details such as the time to extinction of the whole community depend on the initial phenotypic configuration of the community before the onset of environmental change, and on the direction of the CCC motion in phenotype space. In particular, the time to extinction can be highly variable for a

given rate of environmental change. Based on this, one would expect that real ecosystems also exhibit very different times to extinction despite a uniform environmental tendencies, such as global warming.

Some observations made in the simulations were unexpected. In our simulations, communities started their adaptation to environmental change, i.e., to the motion of CCC, from a state of evolutionary equilibrium, and such equilibrium systems can be divided into two groups, high- and low-saturation systems. The first group evolves dense crystal-like configurations of phenotypes with large numbers of species and vanishing phenotypic dynamics at the end of the process of diversity saturation, i.e., at evolutionary equilibrium before the onset of gradual environmental change. In contrast, low-saturation communities have fewer species after settling into the stationary state, and on that state evolution still occurs in the form of oscillating dynamics in phenotype space. The first unexpected result was that for such low-saturation systems, environmental changes that occur at relatively low rates can be a driver of further diversification, leading to an increase in the number of species and to higher phenotypic variation in the community. The result of increased diversity due to environmental change is reminiscent of observations made during a morphological analyses of skulls of two species of mice during the last 50 years in Southern Québec (Roy-Dufresne et al. 2013; Millien et al. 2017). These two species were always very close morphologically, but during the last 15 years they were forced to move further north to a cooler climate, which resulted in adaptation to feeding on different types of grains, morphological divergence of skulls, and a change in the ratio of their population sizes. For a long time one group was more successful, but now the other one appears to become the superior competitor. In this example changes in the abiotic environment lead to an increase in phenotypic variance between the two species and changed competitive interactions, which could potentially lead to different community composition in the future.

Another unexpected observation was that the evolutionary speed can be higher for larger rates of environmental change, even after controlling for adaptation to the moving CCC, Figs. 3F and 5. The adaptive dynamics of species that survived the environmental change predicts that those species exhibit fast but small-amplitude oscillations relative to the moving CCC, which result in the observed increase in evolutionary speed (see videos in Fig. S4). Such patterns of evolutionary phenotypic dynamics have been observed in the fossil record: an analysis of 450 fossil time series indicates that such small-amplitude phenotypic changes translate into quite significant evolutionary speed when measured with sufficient time resolution even though the net phenotypic change over a long period of time is small (**voje2016tempo**). These patterns could also be of interest in the context of comparing the population genetics of populations inhabiting different environments. For example, in a recent study of the wide-spread yellow warbler (Bay et al. 2018), it has been shown that there is a strong association between the frequency of single-nucleotide-substitutions and the rate of environmental change. An increased level of substitutions was observed in genes associated with migration and exploratory behaviour, which can be interpreted as adaptation to environmental change per se (i.e., to the moving CCC in our models), because migration is an efficient way to respond to environmental change. However, in other genes there was a higher level of nucleotide substitutions as well (Bay et al. 2018). Moreover, numerous studies in bacteria, yeast and plants have shown that higher frequency of mutations can appear as a response to environmental stress (Belavkin et al. 2014; Baym et al. 2016; Maharjan and Ferenci 2017).

The increase in evolutionary rates with faster environmental changes observed here can be understood based on our the earlier work on related models (Doebeli and Ispolatov 2017), where we have shown that communities with fewer species tend to evolve at higher rates. In the present models, faster environmental changes lead to larger decreases in the number of species, and hence to increased evolutionary rates. Nevertheless, this result is somewhat in contrast to other recent and related work for single species evolution in changing environments (Rego-Costa et al. 2018), in which environmental changes were also implemented as the motion of the centre of the carrying capacity, but that motion was allowed to be oscillatory, representing seasonal or generally periodic environmental forcing. This work, which is based on the same competition models used here, has shown that faster environmental forcing makes the evolutionary dynamics of solitary species less chaotic or more predictable than it would be without forcing, with the evolving population essentially being entrained by the motion of the centre of carrying capacity. However, (Rego-Costa et al. 2018) did not allow for diversification, and hence did not study evolutionary dynamics in a community of coevolving species. Here we have not studied in detail the complexity of trajectories of multiple coevolving species, we nevertheless observed that apart from the inevitable tracking of the centre of carrying capacity, evolutionary rates can be elevated due to environmental changes even when one controls for the rate at which the environment changes.

There is a simple empirical evidence that environmental changes affect evolution, but such effects can only be observed on short time scales in empirical systems. Our simulations expand this time horizon at least in the sense that they point out how diverse scenarios of adaptation in changing environments can be in principle. The work presented here complements previous studies of macroevolutionary process (Doebeli and Ispolatov 2014, 2017) by showing that environmental changes can have important and sometimes unexpected consequences for long-term evolutionary dynamics. An interesting aspect of our models is that evolving communities that have become less diverse due to gradual environmental change may rediversify and reach previous saturation levels if the environment ceases to change. However, if that happens the new phenotypic and genealogical composition of the community may be very different from the composition of the community that existed before the environmental change was initiated. Finally, it is worth noting that environmental changes could in principle lead to more

cataclysmic evolutionary changes, such as the evolution of entirely novel phenotypes, which in our models would correspond to an increase in the dimensionality of phenotype space. Such environmental changes would then likely generate new bouts of rapid diversification leading to saturated communities occupying higher dimensional phenotype spaces.

Data Accessibility: codes and averaged results of simulations are available at `https://github.com/EvgeniiaAlekseeva/Climate`.

References

Geritz, Stefan AH, Géza Mesze, Johan AJ Metz, et al. (1998). "Evolutionarily singular strategies and the adaptive growth and branching of the evolutionary tree". In: *Evolutionary ecology* 12.1, pp. 35–57.

Diekmann, Odo (2002). "A beginners guide to adaptive dynamics". In: *Summer School on Mathematical Biology*, pp. 63–100.

Griggs, David J and Maria Noguer (2002). "Climate change 2001: the scientific basis. Contribution of working group I to the third assessment report of the intergovernmental panel on climate change". In: *Weather* 57.8, pp. 267–269.

LaJeunesse, T (2002). "Diversity and community structure of symbiotic dinoflagellates from Caribbean coral reefs". In: *Marine Biology* 141.2, pp. 387–400.

Baker, Andrew C (2003). "Flexibility and specificity in coral-algal symbiosis: diversity, ecology, and biogeography of Symbiodinium". In: *Annual Review of Ecology, Evolution, and Systematics* 34.1, pp. 661–689.

Baker, Andrew C et al. (2004). "Coral reefs: corals' adaptive response to climate change". In: *Nature* 430.7001, p. 741.

Little, Angela F, Madeleine JH Van Oppen, and Bette L Willis (2004). "Flexibility in algal endosymbioses shapes growth in reef corals". In: *Science* 304.5676, pp. 1492–1494.

Guillemain, Matthieu et al. (2005). "Long-term climatic trend and body size variation in teal Anas crecca". In: *Wildlife Biology* 11.2, pp. 81–88.

Yom-Tov, Yoram and Jonathan Yom-Tov (2005). "Global warming, Bergmann's rule and body size in the masked shrew Sorex cinereus Kerr in Alaska". In: *Journal of Animal Ecology* 74.5, pp. 803–808.

Yom-Tov, Yoram and Shlomith Yom-Tov (2006). "Decrease in body size of Danish goshawks during the twentieth century". In: *Journal of ornithology* 147.4, pp. 644–647.

Gienapp, Phillip et al. (2008). "Climate change and evolution: disentangling environmental and genetic responses". In: *Molecular ecology* 17.1, pp. 167–178.

Yom-Tov, Yoram, Noam Leader, et al. (2010). "Temperature trends and recent decline in body size of the stone marten Martes foina in Denmark". In: *Mammalian Biology-Zeitschrift für Säugetierkunde* 75.2, pp. 146–150.

Gardner, Janet L et al. (2011). "Declining body size: a third universal response to warming?" In: *Trends in ecology & evolution* 26.6, pp. 285–291.

Norberg, Jon et al. (2012). "Eco-evolutionary responses of biodiversity to climate change". In: *Nature Climate Change* 2.10, p. 747.

Northfield, Tobin D and Anthony R Ives (2013). "Coevolution and the effects of climate change on interacting species". In: *PLoS biology* 11.10, e1001685.

Roy-Dufresne, Emilie et al. (2013). "Poleward expansion of the white-footed mouse (Peromyscus leucopus) under climate change: implications for the spread of Lyme disease". In: *PLoS One* 8.11, e80724.

Belavkin, Roman V et al. (2014). "Mutation rate plasticity in rifampicin resistance depends on Escherichia coli cell–cell interactions". In: *Nature communications* 5, p. 3742.

Doebeli, Michael and Iaroslav Ispolatov (2014). "Chaos and unpredictability in evolution". In: *Evolution* 68.5, pp. 1365–1373.

Botero, Carlos A et al. (2015). "Evolutionary tipping points in the capacity to adapt to environmental change". In: *Proceedings of the National Academy of Sciences* 112.1, pp. 184–189.

Yvon-Durocher, Gabriel et al. (2015). "Five years of experimental warming increases the biodiversity and productivity of phytoplankton". In: *PLoS biology* 13.12, e1002324.

Baym, Michael et al. (2016). "Spatiotemporal microbial evolution on antibiotic landscapes". In: *Science* 353.6304, pp. 1147–1151.

Gynther, Ian, Natalie Waller, and Luke K-P Leung (2016). *Confirmation of the extinction of the Bramble Cay melomys Melomys rubicola on Bramble Cay, Torres Strait: results and conclusions from a comprehensive survey in August-September 2014*. Queensland Government.

Ispolatov, Iaroslav, Vaibhav Madhok, and Michael Doebeli (2016). "Individual-based models for adaptive diversification in high- dimensional phenotype spaces". In: *Journal of theoretical biology* 390, pp. 97–105.

Laskar, Amzad H, Sasadhar Mahata, and Mao-Chang Liang (2016). "Identification of anthropogenic CO2 using triple oxygen and clumped isotopes". In: *Environmental science & technology* 50.21, pp. 11806–11814.

Obbard, Martyn Ernest et al. (2016a). "Trends in body condition in polar bears (Ursus maritimus) from the Southern Hudson Bay subpopulation in relation to changes in sea ice". In: *Arctic Science* 2.1, pp. 15–32.

— (2016b). “Trends in body condition in polar bears (Ursus maritimus) from the Southern Hudson Bay subpopulation in relation to changes in sea ice”. In: *Arctic Science* 2.1, pp. 15–32.

Doebeli, Michael and Iaroslav Ispolatov (2017). “Diversity and coevolutionary dynamics in high-dimensional phenotype spaces”. In: *The American Naturalist* 189.2, pp. 105–120.

Maharjan, Ram P and Thomas Ferenci (2017). “A shifting mutational landscape in 6 nutritional states: Stress-induced mutagenesis as a series of distinct stress input–mutation output relationships”. In: *PLoS biology* 15.6, e2001477.

Millien, Virginie et al. (2017). “Rapid morphological divergence in two closely related and co-occurring species over the last 50 years”. In: *Evolutionary Ecology* 31.6, pp. 847–864.

Smith, Edward G et al. (2017). “Genetic structure of coral-Symbiodinium symbioses on the world’s warmest reefs”. In: *PloS one* 12.6, e0180169.

Whiteman, John P et al. (2017). “Polar bears experience skeletal muscle atrophy in response to food deprivation and reduced activity in winter and summer”. In: *Conservation physiology* 5.1.

Bay, Rachael A et al. (2018). “Genomic signals of selection predict climate-driven population declines in a migratory bird”. In: *Science* 359.6371, pp. 83–86.

Griffen, Blaine D (2018). “Modeling the metabolic costs of swimming in polar bears (Ursus maritimus)”. In: *Polar Biology* 41.3, pp. 491–503.

Grottoli, Andréa G et al. (2018). “Coral physiology and microbiome dynamics under combined warming and ocean acidification”. In: *PloS one* 13.1, e0191156.

Pagano, AM et al. (2018). “High-energy, high-fat lifestyle challenges an Arctic apex predator, the polar bear”. In: *Science* 359.6375, pp. 568–572.

Pogoreutz, Claudia et al. (2018). “Dominance of Endozoicomonas bacteria throughout coral bleaching and mortality suggests structural inflexibility of the Pocillopora verrucosa microbiome”. In: *Ecology and evolution* 8.4, pp. 2240–2252.

Rego-Costa, Artur, Florence Debarre, and Luis-Miguel Chevin (2018). “Chaos and the (un) predictability of evolution in a changing environment”. In: *Evolution* 72.2, pp. 375–385.

Tseng, Michelle et al. (2018). “Decreases in beetle body size linked to climate change and warming temperatures”. In: *Journal of Animal Ecology*.

Appendix

1. Simulation procedure

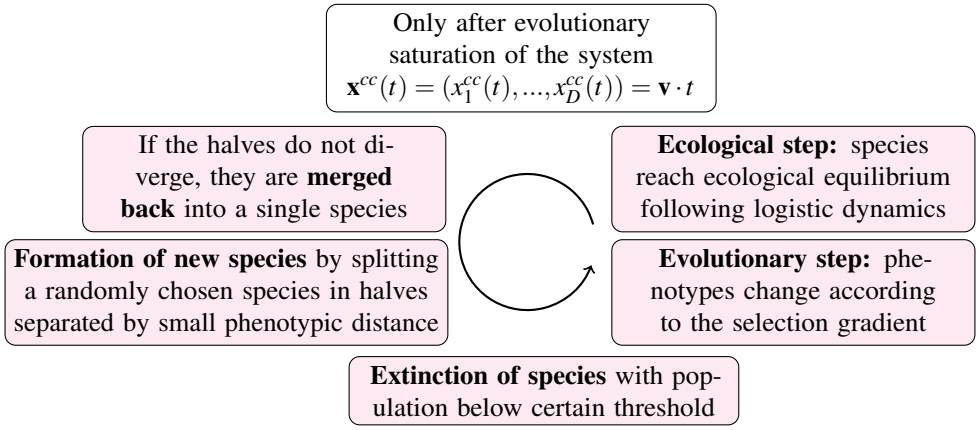

Figure S1. Successive steps that are iterated in the simulations. Each iteration represents a small interval of evolutionary time. The merging and splitting steps are performed once every 10 time units. Movement of CCC starts only after the system comes to a saturation steady state.

Simulations go through a cycle of successive steps, where each iteration corresponds to a small segment of evolutionary time (Fig. S1). An iteration starts with the ecological dynamics, where all species reach their ecological equilibrium according to the logistic dynamics (Eq. 3). Evolutionary time stays constant during this step. If a species crosses the low population limit set equal to 10^{-6}, it is assumed to be extinct and is dropped from the system. In the next step the phenotypes of all species present evolve according to the adaptive dynamics specified in Eq. 6. Phenotypic changes in a single evolutionary time step $\delta t \sim 10^{-2}$ are small enough to keep populations close to their ecological equilibrium (calculated in the previous step).

To model diversification, each 10 time units we split a randomly chosen species in halves separated by a very small phenotypic distance (10^{-3}). If conditions are favorable for evolutionary branching, the distance between halves grows as a result of phenotypic dynamics, and the two "halves" become two sepatrate species. Otherwise, i.e., if the competitive interactions do not favor diversification and the halves do not move apart phenotypically, we merge them back without any consequences to system behavior. Both procedures of merging and splitting happen regularly every few iterations (in this order, so that split halves have time to diverge). If other species come close in phenotypic distance at the moment of merging, they are merged as well.

An evolving system starts a single species with a phenotype tha is randomly chosen from a Gaussian distribution with width 1 and mean 0. The evolutionary equilibration time t^* is defined as the time it takes the system to evolve from a single species to saturation. t^* quickly grows with the dimension of phenotypic space (Fig. S2). The procedure of evolving a system to saturated diversity is described in details in (Doebeli and Ispolatov 2017) in the main text.

In the principal part of our simulations, we analyzed how saturated systems adapt to environmental changes, moving the center of the carrying capacity with various speeds V_C and observing the changes in the systems over an evolutionary time

period equal to t^* or until all species become extinct. The duration t^* was chosen to be the same as the time to system saturation before the onset of environmental change. If a system survives the effects of CCC motion for the time t^*, it usually means that it reaches a new evolutionary steady state adapted to the gradual environmental change.

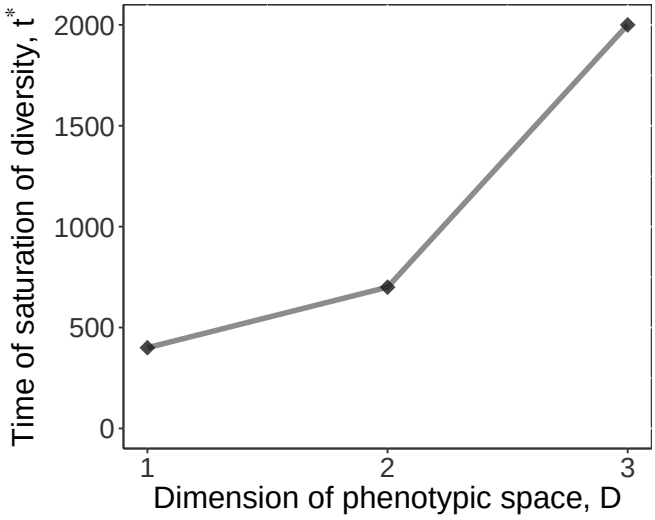

Figure S2. Number of iterations t^* required for system saturation starting from the initial condition of one randomly located species. Around the time t^*, the number of species m_{tot} equilibrates .

The range of CCC velocities was capped using the following simple analytical estimate. If we ignore the asymmetric part of the competition kernel represented by the random coefficients b_{ij} in Eq. (6), which could either reduce or increase the strength of competition in a generally unpredictable way, the remaining adaptive dynamics becomes quite simple. The evolutionary speed **u** has components

$$u_i \equiv \frac{\partial x_i}{\partial t} = -K(\mathbf{x})(x_i - x_{ci})^3. \tag{1}$$

Here we have taken into account that the ecologically-equilibrated single-species population is equal to the corresponding carrying capacity. Assuming for simplicity that the CCC moves along the first phenotypic coordinate, we look for the maximum of u_1, differentiating (1) with respect to $x_i - x_{ci}$. The maximum is achieved at $x_{c1} - x_1 = 3^{\frac{1}{4}}$, and the corresponding maximum evolutionary speed $V_{ev}/lequ_{max} \approx 1.08$. This sets the upper limit on the sustainable velocity of CCC, which results from a competition between two trends: A faster motion of CCC makes the species to trail further behind in phenotype space, thus generating a larger selection gradient. However, the further a species trails behind the CCC, the lower is its population, which makes mutations more rare. Competition between these two trends defines the maximum velocity at which the single species can evolve, which, in other words, is the maximum velocity of CCC that a species can follow at a steady state. In reality, as we will see below, due to the action of asymmetric terms in the competition kernel and due to interspecies competition, all species go extinct well below this maximum CCC velocity.

2. Visualized simulation runs and its parameters

(a) Example of Highly-Saturated System **(b)** Example of Low-Saturated System

Figure S3. Visualisatio of system saturation in two-dimensional phenotypic space, $\sigma_K = 1, \sigma_{i=\{1,\dots,D\}} = 0.5$. Here and in the next figure dark grey circles show the location of different species in phenotype space, with the size of the circles representing the populations sizes, the red circle shows the location of the CCC.

Visualized simulations, presented on Fig.1 and Fig.2 and here on Fig, S4, have following parameters and initial conditions:

A: Highly-saturated system

Simulations start from a single species with population $N = [0.3]$ and phenotypic coordinates

$$\mathbf{x} = \begin{bmatrix} -0.1070 & 1.4071 \end{bmatrix},$$

$$b = \begin{bmatrix} 0.5129 & 0.5054 \\ -0.0446 & -0.1449 \end{bmatrix}.$$

B: Low-saturated system

Simulations starts from single species with population $N = [0.3]$ and phenotypic coordinates

$$\mathbf{x} = \begin{bmatrix} -0.2555 & 1.3599 \end{bmatrix},$$

$$b = \begin{bmatrix} 0.1680 & -0.7389 \\ -0.4749 & 0.6829 \end{bmatrix}.$$

Visualized simulations, presented in Fig.4 and Fig.5 and here on Fig. S4, have following parameters and initial conditions:

A: Highly-saturated system.

Simulations starts from $m = 9$ species with populations

(a) Example of Highly-Saturated System **(b)** Example of Low-Saturated System

Figure S4. Visualisation of system adaptation in two-dimensional phenotypic space, $\sigma_K = 1, \sigma_{i=\{1,\ldots,D\}} = 0.5$.

$N = \begin{bmatrix} 0.4438 & 0.4548 & 0.4836 & 0.4973 & 0.4557 & 0.4658 & 0.5001 & 0.4694 & 0.4831 \end{bmatrix}$ and phenotypic coordinates

$$\mathbf{x} = \begin{bmatrix} -0.0032 & 0.0009 \\ -0.1526 & 0.8647 \\ -0.6074 & -0.9155 \\ 0.8925 & -0.8185 \\ 0.1553 & -0.8632 \\ -0.7655 & -0.0483 \\ -0.8908 & 0.8162 \\ 0.7631 & 0.0449 \\ 0.6086 & 0.9154 \end{bmatrix},$$

$$b = \begin{bmatrix} -0.4474 & -0.6208 \\ 0.2777 & 0.1053 \end{bmatrix}.$$

B: Low-saturated system.

Simulations starts from $m = 2$ species with populations $N = \begin{bmatrix} 0.9179 & 0.9178 \end{bmatrix}$ and phenotypic coordinates

$$\mathbf{x} = \begin{bmatrix} 0.5069 & 0.2021 \\ -0.5057 & -0.1860 \end{bmatrix},$$

$$b = \begin{bmatrix} -0.4796 & 0.7780 \\ -0.6584 & -0.4313 \end{bmatrix}.$$

3. Threshold value of V_C

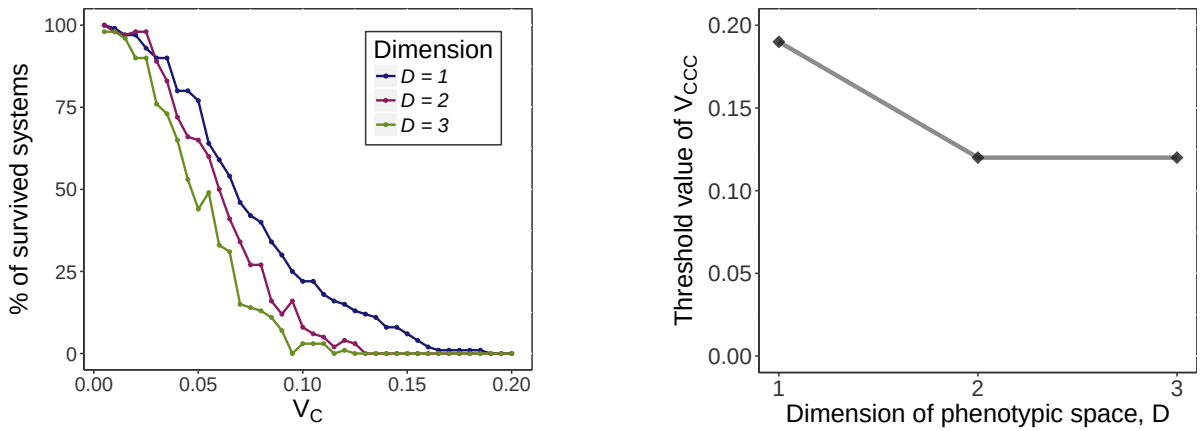

Figure S5. Left panel: The fraction of systems with at least one surviving species from the sample of 100 saturated systems vs. the speed of CCC motion for 3 dimensions of phenotypic space. Right panel: The threshold value of V_C that results in extinction in all 100 replicas vs. dimension of the phenotypic space.

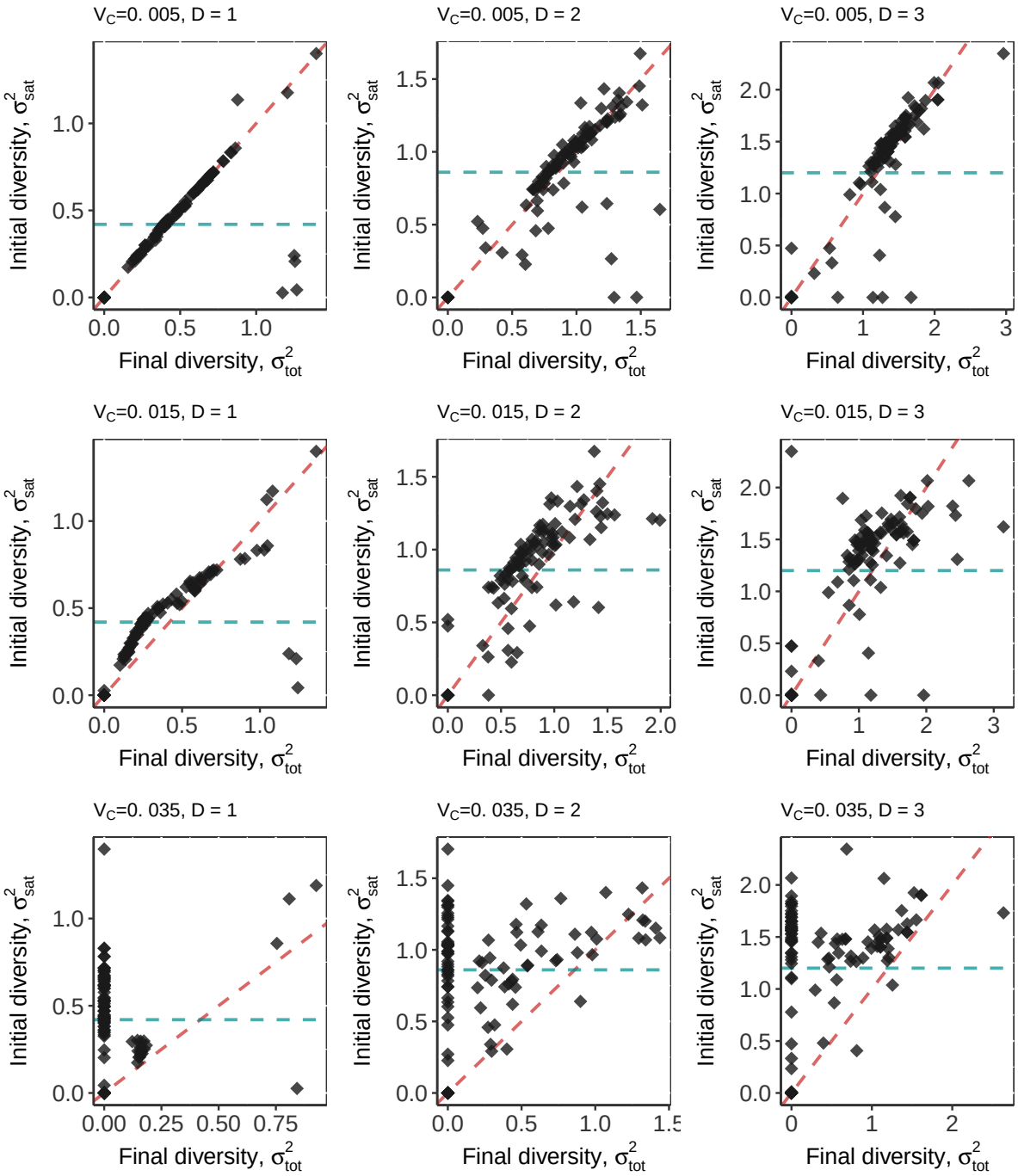

Figure S6. Diversity of saturated systems σ^2_{sat} before the onset of environmental change vs. final diversity σ^2_{tot} present t^* time units after the onset of environmental change. The blue line represents the average saturation level. Points below the red diagonal represent systems in which σ^2_{tot} becomes larger than σ^2_{sat}. Points with zero final diversity represent systems that went extinct.